The lattice dynamics of α- and γ-Ce: a first-principles approach

2007 J. Phys.: Condens. Matter 19 476206

(http://iopscience.iop.org/0953-8984/19/47/476206)

IOP PUBLISHING JOURNAL OF PHYSICS: CONDENSED MATTER

J. Phys.: Condens. Matter **19** (2007) 476206 (12pp) doi:10.1088/0953-8984/19/47/476206

The lattice dynamics of α- and γ-Ce: a first-principles approach

Li Huang[1] **and Chang-An Chen**

State Key Laboratory for Surface Physics and Chemistry, PO Box 718-35, Mianyang 621907, Sichuan, People's Republic of China

E-mail: huangli712@yahoo.com.cn

Received 16 May 2007, in final form 10 October 2007
Published 31 October 2007
Online at stacks.iop.org/JPhysCM/19/476206

Abstract

An *Ab initio* pseudopotentials plane wave method supplemented with the linear response approach has been employed to study the lattice dynamics of face-centered cubic (fcc) α- and γ-cerium. The bulk properties, entire phonon dispersions, phonon density of states, and temperature-dependent thermodynamic quantities of both cerium phases are obtained. With regard to the phonon spectrum of α-Ce, it exhibits imaginary phonon frequencies near the Γ point, indicating that this phase is unstable under low ambient pressure. The calculated phonon spectrum and elastic constants of γ-Ce successfully reproduce several extraordinary features, including pronounced phonon softening at the L point, particularly low energy phonons along the T[$\xi\xi\xi$] branch, and large elastic anisotropy. Some apparent discrepancies have been observed between the phonon density of states of α- and γ-Ce. As a result, the phonon entropy change across the α–γ phase boundary is not negligible. To obtain a full understanding of the driving force of the fascinating α–γ phase transition, the lattice contribution should be taken into consideration.

(Some figures in this article are in colour only in the electronic version)

1. Introduction

Cerium metal, with its 4f electron near the boundary between itinerant and localized behaviors, is an archetypal material in the study of strongly interacting f-electron systems. It has a complex phase diagram, involving several different lattice structures, and varying magnetic and superconducting behaviors. It exhibits the well known α–γ isostructural phase transition characterized by an unusually large volume change [1] of $\sim$15% at room temperature. Numerous theoretical and experimental efforts have been devoted to explain this anomalous phenomenon. To address this problem several hypotheses have been advanced, but the detailed

[1] Author to whom any correspondence should be addressed.

mechanism underlying this phase transition is still the subject of debate. It is generally believed that this transition arises from changes in the degree of 4f electron correlation, as is reflected in both the Mott transition (MT) [2] and Kondo volume collapse (KVC) [3, 4] models.

In the MT scenario [2], the 4f electron is treated to be localized and non-binding in the γ phase, but itinerant and binding in the α phase. Thus the energy for the phase transition is provided by the kinetic energy of the itinerant f electron. Whereas in the KVC picture [3, 4] the 4f electron is assumed to be localized in both the α and γ phases, and the phase transition is driven by the Kondo spin fluctuation energy and entropy. These early models ignore an explicit treatment of the lattice degrees of freedom altogether; even the lattice vibrational entropy is not considered at all. However, the role lattice degrees of freedom play in the α–γ phase transition of cerium remains a mystery.

Inelastic neutron scattering (INS) techniques have been used to investigate the lattice and spin dynamics of γ-Ce [5, 6]. The phonon spectrum of γ-Ce is in general soft, in particular the low frequency phonon branch T[$\xi\xi\xi$]. The elastic constants have been evaluated by a standard Born–von Kármán analysis. It is remarkable that the values of C_{11} and C_{44} are comparable, which is exceptional for a normal metal in fcc structure. With the exception of γ and δ phases, to our best knowledge, the phonon spectra of α and β phases have not been determined by experiments in the publications. We note that the relative importance of spin fluctuation and lattice vibrational contributions to the driving force of the α–γ phase transition is currently under debate, with very different conclusions reached from successive experimental studies of the $Ce_{0.9}Th_{0.1}$ alloy [7] and pure cerium [8]. Manley *et al* [7] have measured the phonon density of states (DOS) of the $Ce_{0.9}Th_{0.1}$ alloy at 150 K (γ phase) and at 140 K (α phase) using INS techniques, which show little difference between the α and γ phases. As a result it is proposed by Manley *et al* that the lattice vibrational entropy change in the phase transition can be safely neglected. By contrast, in a subsequent experiment [8] the temperature and pressure dependence of the thermal displacements and lattice parameters of pure Ce are obtained across the α–γ phase transition by using high pressure, high resolution neutron and synchrotron x-ray powder diffraction. The estimated vibrational entropy change per atom in the phase transition is about half of the total entropy change, which clearly demonstrates the importance of lattice vibrations in addition to the spin and charge degrees of freedom for a complete description of the α–γ phase transition.

Theoretical works which are concerned with the lattice dynamics of Ce are also very limited. Min *et al* [9] have evaluated the Stoner factor and electron–phonon coupling parameters of α- and γ-Ce, using a total energy full-potential linearized augmented plane wave method. They speculate that some anomalies may be seen in the phonon spectrum which are associated with a possible softening in the transition arising from the electronic contribution, and the electron–phonon interaction should play an important role during the α–γ phase transition. Recently, Amadon *et al* [10] emphasized, on the basis of experimental data and dynamical mean field theory calculations, that the entropic stabilization of the γ phase is the main driving force of the α–γ transition of cerium over a wide range of temperatures below the critical point. Notably, no theoretical phonon spectra of Ce from first-principles have been available until the present time, which has been mainly attributed to the competitive behavior between localization and itinerancy in the 4f electron of Ce. Once available, the comparison of phonon spectra in various phases of Ce metal will yield crucial insights into the nature of the phase transition as well as other unusual features.

Clearly, to understand the novel properties of Ce hinges on the ability to obtain highly reliable experimental data and theoretical results. Of these, the lattice dynamical properties, especially the phonon dispersion relations, are key to the elucidation of phase transitions among multiple allotropic forms and other intriguing properties of Ce. Unfortunately, as introduced

above, both experimental and theoretical knowledge about the lattice dynamical properties of this element have so far been insufficient. Hence this paper is intended to shed new light on the first-principles calculations of bulk and lattice dynamical properties of the α- and γ-Ce, stressing the interrelationship among the elasticity, phonon, vibrational entropy, and phase stability of Ce. The lattice dynamics of β and δ-Ce will be taken into account in our next paper.

This paper is organized as follows. In the next section we describe the theoretical methods briefly. The *ab initio* determinations of the equilibrium volumes, equations of states, and elastic constants of both cerium phases are discussed and compared to the experiments in sections 3. Section 4 is devoted to analyzing the calculated phonon spectra of α- and γ-Ce in detail. The phonon density of states and vibrational entropy are also presented in section 5. Finally, a summary of the presented results is given in section 6.

2. Computational methodology

Numerous first-principles calculations in regard to the ground state properties of cerium, e.g. total energy, equilibrium volume, electronic structure, and magnetic moment etc, have been reported in the publications. Most of the previous theoretical calculations [9, 11–13] are based on the all electron and full-potential schemes, whereas in the present work, we calculate the phonon band structures for both α and γ phases in arbitrary wavevectors, using the *ab initio* pseudopotentials plane waves method combined with the linear response approach. Recently Savrasov and Kotliar [14] have merged the dynamical mean field theory and linear response theory to investigate the lattice dynamics in strongly correlated systems. Subsequently, Dai *et al* [15] employed this novel method to study the phonon spectra of plutonium (δ and ε phases) at high temperatures. It is astonishing that the calculated results are in good agreement with the later experiments [16, 17]. In contrast to the fashionable dynamical mean field approach, we would like to show that the bulk properties and lattice dynamics of Ce, which is a typical electronic correlated system, could be reasonably reproduced by using the traditional pseudopotentials plane wave method as well.

The following results have been obtained thanks to the use of the ABINIT [18] package. The ABINIT code is based on plane waves and pseudopotentials. The wavefunctions describe only the valence and the conduction electrons, while the core electrons are taken into account using pseudopotentials. In the present work, two Hamann scheme [19] norm conserving pseudopotentials were generated by ourselves thanks to the FHI98PP [20] code. According to the MT scenario [2], the $4f^1$ state of α-Ce is considered as itinerant, whereas the one of γ-Ce is highly correlated, i.e. localized. Consequently, the considered valence electrons for α- and γ-Ce are $4f^1 5s^2 5p^6 5d^1 6s^2$ and $5s^2 5p^6 5d^1 6s^2$, respectively. We treat the [Xe] closed shell as core electrons for α-Ce, and treat the [Xe] closed shell plus a single 4f state as core electrons for γ-Ce. Generally speaking, the latter treatment is not justified within the spirit of the pseudopotential approximation. A pseudopotential is generated from a spherical atom, the charge density associated with a closed shell is spherical while that associated with a single 4f electron is not. Therefore, we presume that the 4f orbitals in γ-Ce are 14-fold degenerate (including spin freedom) such that each is fractionally occupied with a value of $1/14$ electrons. It appears that this spherical averaging of the $4f^1$ state in γ-Ce does result in some qualitative agreement with experiments. In accordance with the literature [21], the cutoff radii are $r_{5s} = 1.29\ a_0$, $r_{5p} = 1.49\ a_0$, $r_{5d} = 1.99\ a_0$, and $r_{4f} = 1.99\ a_0$. In addition, the core electrons are treated within a scalar relativistic formalism and the angular momentum component $l = 0$ is taken as the local part. The parameters we have chosen can be seen as a compromise between transferability and convergence.

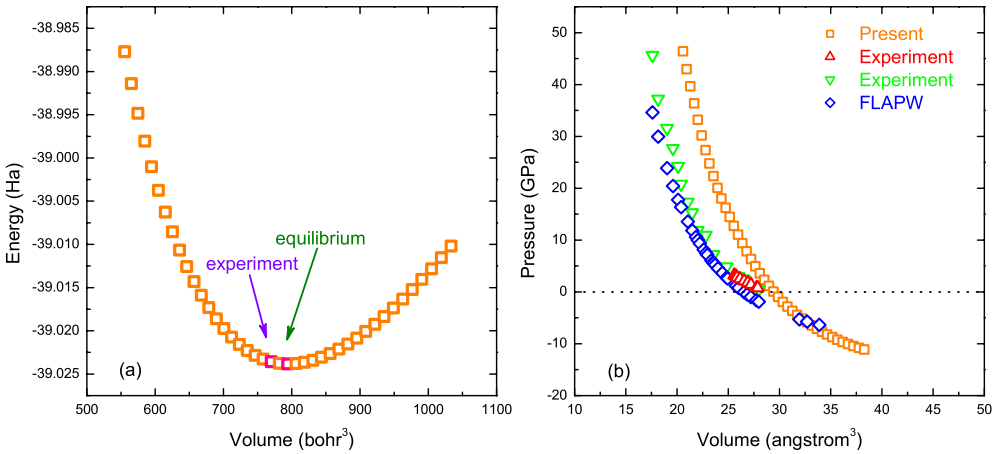

Figure 1. (a) Calculated total energies of α-Ce as a function of volume. (b) Theoretical and experimental equation of states of α-Ce. The experimental data displayed by up and down triangles ($\triangle$ and $\triangledown$) are taken from [23] and [24], respectively. For comparison, we have used the full-potential linearized augmented plane wave code to calculate the p–V curve of α-Ce over a wide range of pressures and volumes. The results are marked with diamonds ($\Diamond$).

Before starting the work on ground state and linear response calculations, a set of convergence tests have been done in order to choose correctly the grid of special k points and the cutoff for the plane waves' kinetic energy. During these tests the grid density and the cutoff energy value have been consecutively and independently increased. We use in the further calculations a plane waves' kinetic energy cutoff of 40 Ha, which is sufficient to fully converge all properties of relevance, and the Brillouin zone integration is confined to $6 \times 6 \times 6$ Monkhorst–Pack wavevector meshes for both α and γ phases. To attain a closer agreement with the experiments, all the calculations have been completed utilizing the generalized gradient approximation (GGA) with the well-established exchange–correlation function proposed by Perdew *et al* [22]. It is worth emphasizing that we have accomplished our theoretical calculations using the finite temperature smearing scheme (as the broadening of orbital occupation numbers is based on Fermi–Dirac statistics) by way of comparing with the experimental results. The temperature of smearing for α-Ce is 0.0005 Ha ($\sim$158 K), and that for γ phase is 0.002 Ha ($\sim$632 K). All the linear response calculations have been carried out at the equilibrium crystal structures, determined by a geometry optimization procedure in advance.

3. Bulk properties

Firstly, we just calculate the equilibrium properties of α- and γ-Ce for the sake of judging whether the computational methodology as described above is reliable and effective.

The calculated total energies and pressures of α-Ce as a function of volume, i.e. $E(V)$ and $P(V)$ curves, together with the corresponding experimental data are plotted in figure 1. The equilibrium volume of the α phase is 793.93 bohr^3, which is only 3.1% larger than the experimental value [1] of 769.88 bohr^3. Less satisfactory, in comparison with the experimental data [23, 24], the present $P(V)$ curve shifts somewhat to the right. Thus the obtained equation of states does not describe the α phase well at high pressure, but becomes progressively better at lower pressure. Figure 2 depicts the energy–volume and pressure–volume relations of γ-

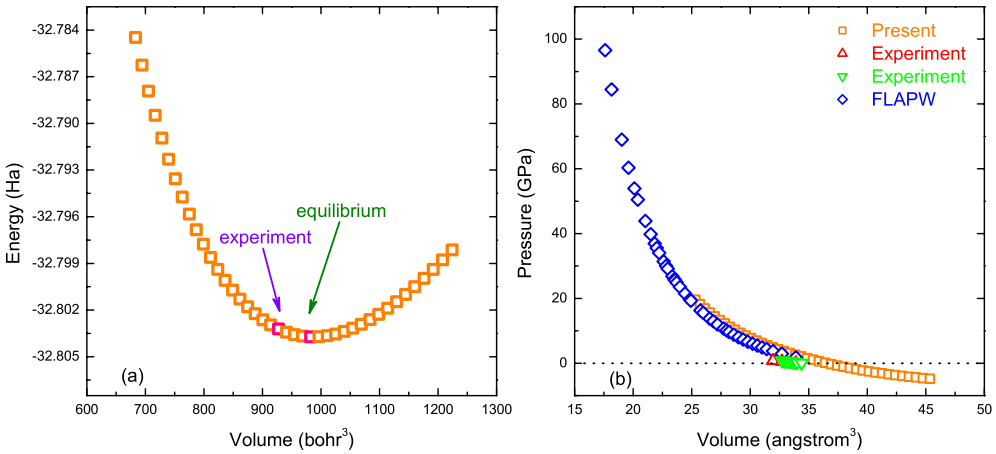

Figure 2. (a) Calculated total energies of γ-Ce as a function of volume. (b) Theoretical and experimental equation of states of γ-Ce. The experimental data are taken from [8] and [24]. The experimental values and full-potential linearized augmented plane wave computational results are represented by various symbols as explained in figure 1.

Table 1. Calculated bulk moduli B, shear moduli C', and elastic constants C_{ij} of α- and γ-Ce along with experimental and other theoretical data. All the quantities listed in this table are in GPa.

	α-Ce			γ-Ce		
	Present	Experiment	Theory	Present	Experiment	Theory
C_{11}	72.6			37.9	24.1[a]	
C_{12}	67.7			26.4	10.2[a]	
C_{44}	4.5			20.9	19.4[a]	
B	69.4	35.0[b]	48.4[c], 48.7[d], 43.0[e]	30.2	14.8[a], 21.0[f]	31.0[c], 29.6[g]
C'	2.4			5.8	7.0	

[a] Reference [5]. [b] Reference [25]. [c] Reference [26]. [d] Reference [12]. [e] Reference [21]. [f] Reference [24]. [g] Reference [13].

Ce. The predicting equilibrium volume of the γ phase is 982.32 bohr^3, in accordance with the experimental value [1] of 927.36 bohr^3 (the error is about 5.9%). The present equation of states of the γ phase is seen to correspond well to the experimental data [8, 24]. Since there are few experimental data left so far, we have calculated the equation of states of the γ phase in a wide range of pressures and volumes by using the full-potential linearized augmented plane wave code, and compared it with the current one. As is expected, the two theoretical curves fit quite well.

By treating homogeneous strain within the framework of linear response theory, direct calculation of the elastic tensors of solids can be accomplished [27]. In the present work, we calculate the elastic constants (C_{ij}) of α- and γ-Ce. Consequently, the bulk modulus B and shear modulus C' are also evaluated by applying $B = (C_{11}+2C_{12})/3$ and $C' = (C_{11}-C_{12})/2$, respectively. We compare the results of our calculations with the limited experimental data [5, 24, 25] in table 1. Other selected theoretical results [12, 13, 21, 26] are collected as well.

As is seen in table 1, the calculated bulk modulus of the α phase is 69.4 GPa, which is almost twice the experimental value of 35.0 GPa [25]. Simultaneously other theoretical results

(48.7 GPa [12] and 43.0 GPa [21]) significantly overestimate the bulk modulus of α-Ce too. Since it is very difficult to prepare a sample of pure α-Ce without any mixing of β-Ce, it is hard to obtain enough and accurate experimental data for α-Ce. For the elastic constants, at present we have no experimental or other theoretical data with which to compare our results, so our data are predictive. It is noticed that C_{11} comes closer to C_{12}, which implies that the α phase will be unstable against small homogeneous deformations. On the other hand, the velocity of a longitudinal wave in the [100] direction is much larger than the one of a shear wave since C_{44} is much smaller than C_{11}. As for γ-Ce, we have reproduced several pronounced unusual features in the elasticity. Firstly, C_{44} is very close to C_{12}, i.e. the deviation from the Cauchy relation ($C_{12} = C_{44}$) is very small, which means that the interatomic forces have a strong noncentral component. Second, the distortion described by C' is quite soft, which highlights a huge anisotropy in the elastic properties of γ-Ce along different directions. Third, C_{44} and C' differ by almost a factor of three [5, 6], though it is smaller than the values found in other unusual fcc metals such as Pu ($\sim$6) [16] and Th (3.6) [28], indicating large anisotropy with regard to the propagation of elastic waves. Obviously the discrepancy between our data and experimental results is not trivial, which may be explained by the inherent limitations of traditional density functional theory (poor treatment of the electronic correlation) and the pseudopotentials approximation. But one may also question somewhat the accuracy of the experimental data. For instance, for the bulk modulus of γ-Ce, data spanning from 0.148 to 0.210 ([5, 24]) have been reported. Therefore further experiments should be undertaken to provide reliable data and critical tests for the theoretical treatments.

4. Phonon band structures

Thanks to the state-of-the-art density functional perturbation theory [29], it is now possible to obtain accurate phonon dispersions on a fine grid of wavevectors covering the entire Brillouin zone, which compare directly with neutron diffraction data, and from which several physical properties of the system (such as heat capacities, free energy, entropy, and so on) can be calculated. Technical details on the computation of dynamical matrices, phonon dispersions, and interatomic force constants can be found in [30] and [31].

Many phase transitions, both those induced by pressure and those induced by temperature, are driven by lattice instability. This may be an elastic instability or a phonon instability [29]. In this section we first concentrate our attention on the relationship between the phonon spectrum and the phase stability of α-Ce. Depicted in figure 3 is the calculated phonon dispersion curves of α-Ce along the high symmetry lines ($\Gamma \longrightarrow$ K $\longrightarrow$ X $\longrightarrow$ Γ $\longrightarrow$ L $\longrightarrow$ X $\longrightarrow$ W $\longrightarrow$ L) of irreducible Brillouin zone (IBZ).

The most interesting feature of the phonon dispersion curves of α-Ce is the occurrence of imaginary phonon frequencies near the Γ point. The transverse acoustic branches T[$\xi\xi\xi$] and T_1[$0\xi\xi$] are unstable at small values of the q vector. It is well known that the imaginary phonon frequencies imply the anharmonic effects and phase instability, thus the lattice vibrations in the α phase are anharmonic and involve large nuclei excursions from their equilibrium positions, i.e. the internal atomic coordinates of the α phase may be unstable. Another interesting aspect of the phonon dispersion curves of α-Ce is the especially low energy transverse acoustic branch T[$\xi\xi\xi$]. The transverse acoustic frequency at the boundary of the IBZ (L point) is only 1.1 THz. Very low energies of the T[$\xi\xi\xi$] branch in an fcc lattice are commonly associated with a distortion that causes an increase in the dimensions of the unit cell, because the low energy modes at the L point suggest that along the [$\xi\xi\xi$] direction each atomic plane could easily slide relative to its immediate neighboring atomic planes to form a new staking arrangement. In previous publications, it was argued that the equilibrium structure of Ce in the ground state

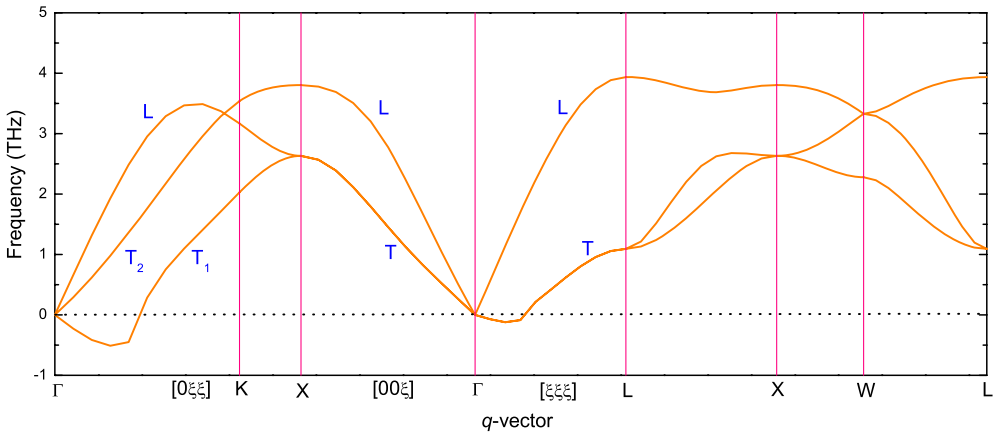

Figure 3. Calculated phonon spectrum of α-Ce in the main symmetry directions. The longitudinal and transverse modes are denoted as L and T, respectively.

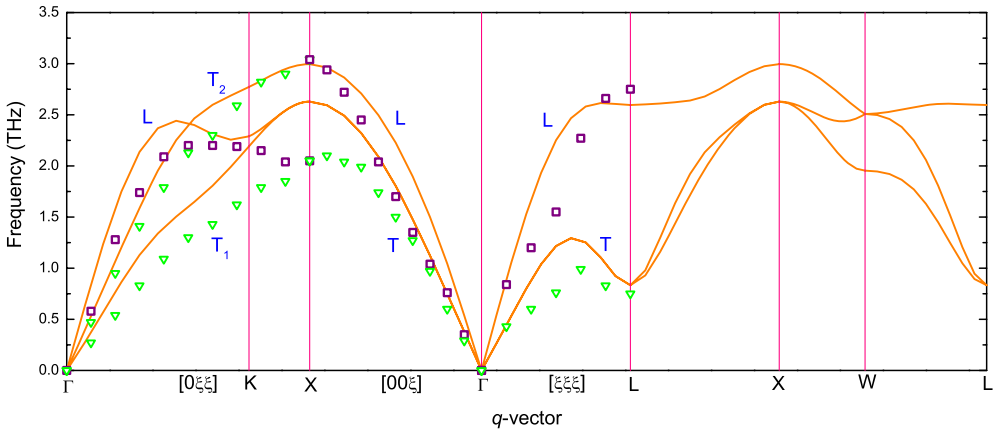

Figure 4. Calculated and experimental phonon spectrum of γ-Ce along high symmetry directions. The experimental data are taken from [5]. The open squares (□) and down triangles (▽) mark the experimental values of longitudinal (L) and transverse (T) modes, respectively.

may be α' phase [11] or α'' phase, [32] instead of α phase. The α' phase resembles a hexagonal close packed (hcp) structure, and the lattice of the α'' phase (with space group $C2/m$) is a distortion of the fcc structure. Since it is convenient to attain the α' or α'' phases through the deformation of the original α phase, it is therefore not surprising that the α–α' or α–α'' phase transitions take place under small ambient pressure. As a matter of fact, even at very low pressure (only 0.7 GPa at 300 K [1]) the α phase can transform to α' or α'' phases. To summarize, we believe that the imaginary phonon frequencies and low energy branch T[$\xi\xi\xi$] are responsible for the phase transitions and stabilization of low symmetry structures.

We now turn to the description of our results for the phonon band structures of γ-Ce (see figure 4). Overall, the phonon frequencies are positive, showing the internal stability of the positions of the nuclear coordinates in γ-Ce. Comparison of the dispersion curves with those of other fcc elements and in particular with those of Th which is in the same column of the periodic table as Ce would have been useful and constructive. Taking the difference in atomic

Table 2. Summary of the most important phonon frequencies of γ-Ce at several high symmetry points of IBZ calculated in the present work. The corresponding experimental data [5, 6] are also collected in this table for comparison.

Phonon mode	Present (THz)	Experimental (THz)
LA(L)	3.06	2.75[a], 2.86[b], 2.80[c]
TA(L)	1.29	0.75[a], 0.82[b], 0.94[c]
LA(X)	3.25	3.04[a], 3.20[b], 3.03[c]
TA(X)	2.41	2.05[a], 2.10[b], 2.00[c]
LA(K)	2.63	2.17[a]
TA_1 (K)	2.07	1.71[a]
TA_2 (K)	2.98	2.71[a]

[a] Reference [5], measured at room temperatures.
[b] Reference [6], measured at 295 K.
[c] Reference [6], measured at 875 K.

masses, lattice constants, and melting points into account, it is evident that the phonon spectrum of γ-Ce is in general softer than that of Th [28]. This phenomenon is particularly pronounced for the longitudinal branches as well as the T[$\xi\xi\xi$] and T_1[$0\xi\xi$] branches. But for the T[00ξ] and T_2[$0\xi\xi$] branches, the lowering of the phonon frequencies is not as pronounced with respect to the corresponding branches of Th. This observation is interesting since the longitudinal and transverse modes along the Δ line ([00ξ]) and T_2[$0\xi\xi$] are the branches whose slopes in the elastic limit involve the elastic constants C_{11}, C_{44}, and C_{12} respectively, which determine the bulk modulus B and shear modulus C' of the materials. The relatively soft phonon spectrum implies that the elasticity of γ-Ce will show anomalous anisotropy as discussed above. There exists another apparent distinction between the phonon spectrum of γ-Ce and that of Th. In the T_1[$0\xi\xi$] and T_2[$0\xi\xi$] branches of Th [28], nonlinear 'kink' structures, i.e. the so-called Kohn anomaly, have been found. Nevertheless, in the phonon spectrum of γ-Ce, it seems that analogous 'kink' structures do not appear.

The most striking feature of the experimental phonon spectrum of the γ phase is a soft mode behavior for the transverse acoustic branch along the Λ line ([$\xi\xi\xi$]). In the preliminary INS measurements, Stassis *et al* [5] claim that there is a soft mode lying in the T[$\xi\xi\xi$] branch, in other words, this branch exhibits a dip near the zone boundary. In their later report [6] they reformulate that close to the border of IBZ (L point), the frequencies of the T[$\xi\xi\xi$] branch exhibit an unusual temperature dependence, increasing with increasing temperatures. As is clearly seen in figure 4, the phonon softening of the T[$\xi\xi\xi$] branch near the zone boundary is well reproduced by our calculations. Similar to the α phase, γ-Ce also has low energy and strongly damped phonons along the T[$\xi\xi\xi$] branch. Pure γ-Ce, on increasing temperature, transforms into the δ phase, which has a body-centered cubic (bcc) structure. If lowering the temperature, the transition leads, instead, to a double hexagonal close packed (dhcp) structure (β phase). Thus it seems that premonitory effects of the transitions are present in the calculated phonon dispersion curves of γ-Ce, and the damped phonons along the T[$\xi\xi\xi$] branch are probably the key features associated with the γ–δ and γ–β transitions.

The phonon frequencies of γ-Ce at high symmetry points of IBZ are summarized in table 2, together with the experimental results [5, 6]. Though theoretical phonon frequencies are slightly larger than those of experiments and the detailed q-dependence of these phonon branches shows some residual discrepancies, as a whole the calculated phonon band structures of the γ phase are in reasonable agreement with experimental results (see figure 1 in [5]). It is fair to state that most of the important features of the phonon properties of γ-Ce have been reproduced by our first-principles calculations, e.g. soft phonon dispersions, phonon

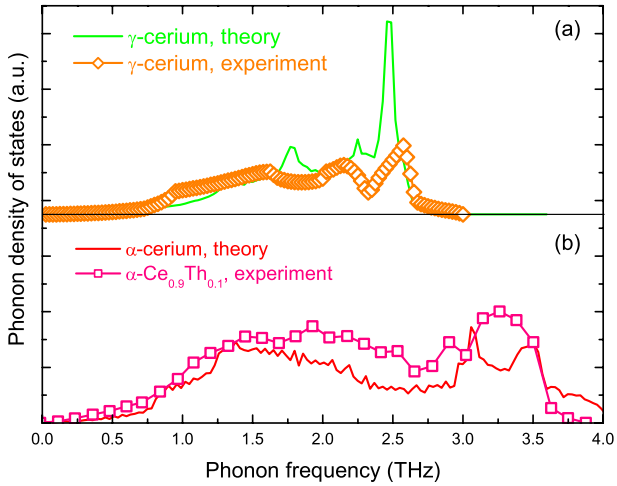

Figure 5. Calculated and experimental phonon DOS of α-Ce, α-$Ce_{0.9}Th_{0.1}$, and γ-Ce. The experimental data of the α-$Ce_{0.9}Th_{0.1}$ alloy (open squares) are obtained at 10 K, reproduced from [7]. And the experimental data for γ-Ce (open circles) are measured at room temperature, reproduced from [5]. The dashed and solid lines represent the calculated phonon DOS of pure α and γ phases, respectively.

softening at the L point, damped phonons in the T[$\xi\xi\xi$] branch, nonexistent Kohn anomaly, etc. The divergence of theoretical results and experiments is probably caused by the effects of temperature and strongly correlated 4f electron.

5. Phonon density of states and vibrational entropy

As a byproduct, we also determine the phonon DOS of α and γ phases. Both calculated phonon DOS, together with the relevant experimental data are illustrated in figure 5. Stassis *et al* [5] have measured the phonon DOS of γ-Ce at room temperatures, and those of α-$Ce_{0.9}Th_{0.1}$ alloy at 10, 100, and 140 K were determined recently by Manley *et al* [7]. Yet the phonon DOS of pure α phase has not been attained so far.

As evident in figure 5, the discrepancy of phonon DOS between α and γ phases is not ignorable. In the high frequency region (>3.0 THz), α-Ce has relatively high occupation, nevertheless, the occupation of γ-Ce tends zero. Because our calculations based on linear response theory and harmonic approximation yield imaginary phonon frequencies at small q vector in the phonon spectrum of the α phase, it is not strange that in the corresponding phonon DOS there exists a sharp peak located near zero frequency (not shown in the figure). On the contrary, concerning the phonon DOS of γ-cerium, such a peak is absent. To sum up, there is essentially a significant change in the calculated phonon DOS across the α–γ phase boundary, which causes the noticeable vibrational entropy change $\Delta S_{\rm vib}^{\alpha-\gamma}$.

The knowledge of the entire phonon dispersion curves and DOS make possible the evaluation of several critical thermodynamical quantities and of the relative stability of the system among different crystal structures. Using the phonon frequencies and DOS reported above, the temperature-dependent phonon contribution to the Helmholtz free energy $F(T)$ and entropy $S(T)$ are computed. From $F(T)$ and $S(T)$, any other thermodynamical property can be accessed conveniently. In this work, thermodynamical quantities with temperature, including $F(T)$, $S(T)$, and constant pressure specific heat $C_p(T)$ of α- and γ-cerium are treated properly.

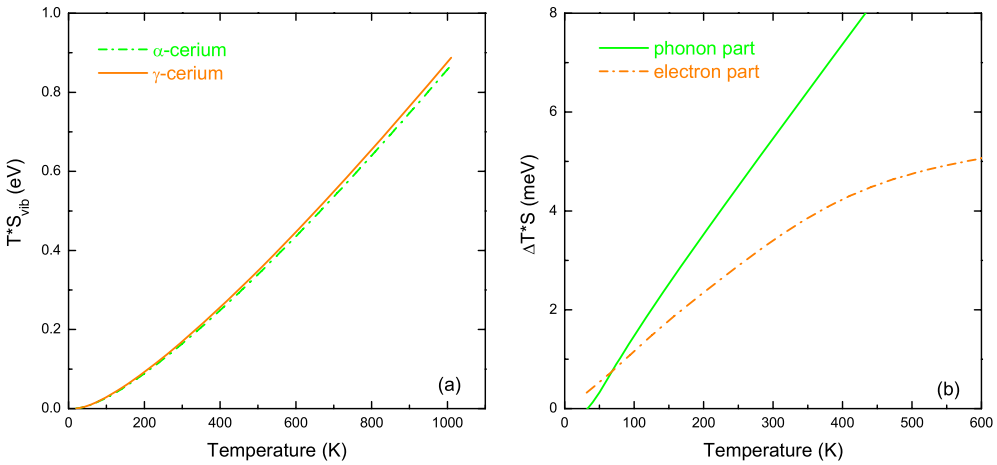

Figure 6. (a) Calculated vibrational entropy of α- (dashed) and γ-Ce (solid line) as a function of temperature. (b) Temperature-dependent vibrational entropy change ($\Delta S_{\rm vib}^{\alpha-\gamma}$, solid line) and electronic entropy change ($\Delta S_{\rm electron}^{\alpha-\gamma}$, dashed). The electronic entropy can be easily accessed through the decomposition of total energy in a ground state calculation.

The temperature-dependent phonon entropy of both cerium phases are plotted in figure 6(a). On the other hand, the decomposition of the total energy in the ground state calculation can be utilized to evaluate the electronic entropy with temperature. We have calculated the vibrational entropy change $\Delta S_{\rm vib}^{\alpha-\gamma}$ and electronic entropy change $\Delta S_{\rm electron}^{\alpha-\gamma}$ with temperature independently. The results are displayed in figure 6(b). As depicted in figure 6(b), with increasing temperature, both vibrational and electronic entropy changes increase. However, the vibrational entropy change is obviously larger than the counterpart of the electron contribution, especially in the high temperature region. It is corroborated that for the α–γ phase transition entropy, the contribution from the phonon entropy must be accounted for, and the lattice vibrations are likely to play an important role in the transition.

Jeong *et al* [8] have studied the pressure dependence of the thermal displacement and bulk modulus of α-Ce and γ-Ce. They conclude that the vibrational entropy, accounting for about half of the total change in entropy at the α–γ transition, is the crucial factor in stabilizing γ-Ce. Our calculated results are consistent with their viewpoints, but not with the analysis of the phonon DOS of $Ce_{0.9}Th_{0.1}$ alloy measured by Manley's group [7]. The latter results from INS studies on $Ce_{0.9}Th_{0.1}$ alloy actually represent no change across the α–γ phase transition despite the $\sim$15% volume change. Therefore it is argued that most of the transition entropy can be accounted for with the crystal field and changes in the ground state spin fluctuations. If taking the difference in lattice constants into consideration, it is obvious that the two phonon DOS are essentially the same; even for high frequency modes. We note that the phonon spectrum of fcc Th is harder than that of γ-Ce. Thus, a few per cent of the Th element is probably necessary to change the lattice dynamical properties of cerium prominently, and lead to the indistinguishable phonon DOS for α- and γ-$Ce_{0.9}Th_{0.1}$ alloy.

6. Concluding remarks

Notwithstanding the considerable attention, there remains continued disagreement about the underlying mechanism and driving force of the α–γ phase transition of cerium. Now the focus

is put on whether the phase transition is entropy-driven and what role lattice vibrations play in the phase transition. To provide a quantitative picture of the lattice contribution to the driving force of the α–γ phase transition, phonon band structures, and phonon related properties, we have employed the *ab initio* pseudopotentials plane wave method and linear response approach to investigate the bulk and lattice dynamical properties of α- and γ-cerium systematically.

The equilibrium volumes and equation of states of α- and γ-Ce have been successfully reproduced. With regard to the elastic constants, our results are not very consistent with the available experimental data. As for α-Ce, C_{11} comes closer to C_{12}, and C_{44} is threefold smaller than C_{11}, implying a soft response of α-Ce to volume conserving tetragonal distortion. The elasticity of γ-Ce highlights an extraordinary anisotropy. The complete phonon dispersion curves of α and γ phases are given. The phonon spectrum of α-Ce displays imaginary frequencies near the center of the IBZ (Γ point), which is totally unexpected. It is suggested that α-Ce is unstable, and easily transforms to other low symmetry structures under small external pressure. Wills *et al* [11] have proposed that the itinerant 4f or 5f electrons favor distorted crystal structures, e.g. α-U, α-Pu, and α'-Ce. Our results are in accordance with their viewpoints. The calculated phonon spectrum of γ-Ce successfully reproduces several extraordinary features which have been reported in earlier experimental investigations [5, 6], including pronounced low frequency and damped phonons along the T[$\xi\xi\xi$] branch and phonon softening near the L point. The soft mode behavior near the L point is probably a key feature associated with the phase transition of γ-Ce. It should be pointed out that a similar soft phonon has been found in δ-Pu [15–17]. The phonon spectrum of α-Ce is harder than that of γ-Ce, thus the phonon DOS of α- and γ-Ce is distinguishable, especially for high frequency modes. We evaluate the temperature-dependent vibrational entropy $S_{\mathrm{vib}}(T)$ for both cerium phases. It is noticeable that the vibrational entropy change can be comparable with the contribution of spin and charge. Finally, we note that our results mean that a complete understanding of the fascinating properties of Ce and its anomalous α–γ transition must take into account the important interactions between the spin, charge, and lattice degrees of freedom.

Cerium metal is a typical material of strongly interacting f-electron systems. It is hard to reproduce its fascinating physical properties completely by using traditional density functional theory. We believe that a better result could have been obtained if some novel methods beyond LDA for describing the complex electron–electron interactions, such as a LDA + U scheme or dynamical mean field theory, had been employed.

Acknowledgments

LH would like to thank Professor Xi Dai for instructive discussions. The authors are grateful to Dr Bingyun Ao, and Peng Shi for their assistance while preparing this paper. This research is sponsored by the Chinese Academy of Engineering Physics under Contract No. SJ2006-03.

References

[1] Koskenmaki D C and Gschneidner K A Jr 1978 *Handbook of Physics and Chemistry of Rare Earths* (Amsterdam: North-Holland) chapter 4 (Cerium)
[2] Johansson B 1974 *Phil. Mag.* **30** 469
[3] Allen J W and Martin R M 1982 *Phys. Rev. Lett.* **49** 1106
[4] Allen J W and Liu L Z 1992 *Phys. Rev.* B **46** 5047
[5] Stassis C, Gould T, McMasters O D, Gschneidner K A Jr and Nicklow R M 1979 *Phys. Rev.* B **19** 5746
[6] Stassis C, Loong C K, McMasters O D and Nicklow R M 1982 *Phys. Rev.* B **25** 6485
[7] Manley M E, McQueeney R J, Fultz B, SwanWood T, Delaire O, Goremychkin E A, Cooley J C, Hults W L, Lashley J C and Osborn R 2003 *Phys. Rev.* B **67** 014103

[8] Jeong I-K, Darling T W, Graf M J, Proffen T and Heffner R H 2004 *Phys. Rev. Lett.* **92** 105702
[9] Min B I, Jansen H J F, Oguchi T and Freeman A J 1986 *Phys. Rev.* B **34** 369
[10] Amadon B, Biermann S, Georges A and Aryasetiawan F 2005 *Preprint* cond-mat/0504732
[11] Wills J M, Eriksson O and Boring A M 1991 *Phys. Rev. Lett.* **67** 2215
[12] Soderlind P, Eriksson O, Trygg J, Johansson B and Wills J M 1995 *Phys. Rev.* B **51** 4618
[13] Shick A B, Pickett W E and Liechtenstein A I 2001 *J. Electron Spectrosc. Relat. Phenom.* **114–116** 753
[14] Savrasov S Y and Kotliar G 2003 *Phys. Rev. Lett.* **90** 056401
[15] Dai X, Savrasov S Y, Kotliar G, Migliori A, Ledbetter H and Abrahams E 2003 *Science* **300** 953
[16] Wong J, Krisch M, Farber D L, Occelli F, Schwartz A J, Chiang T C, Wall M, Boro C and Xu R Q 2003 *Science* **301** 1078
[17] McQueeney R J, Lawson A C, Migliori A, Kelley T M, Fultz B, Ramos M, Martinez B, Lashley J C and Vogel S C 2004 *Phys. Rev. Lett.* **92** 146401
[18] Gonze X, Beuken J M, Caracas R, Detraux F, Fuchs M, Rignanese G M, Verstraete M L S, Zerah G, Jollet F and Torrent M 2002 *Comput. Mater. Sci.* **25** 478
[19] Hamann D R 1989 *Phys. Rev.* B **40** 2980
[20] Fuchs M and Scheffler M 1999 *Comput. Phys. Commun.* **119** 67
[21] Richard N and Bernard S 2001 *J. Alloys Compounds* **323/324** 628
[22] Perdew J P, Burke K and Ernzerhof M 1996 *Phys. Rev. Lett.* **77** 3865
[23] Zachariasen W H and Ellinger F H 1977 *Acta Crystallogr.* A **33** 155
[24] Olsen J S, Gerward L, Benedict U and Itié J P 1985 *Physica* B+C **133B** 129
[25] Olsen J S, Gerward L, Dancausse J P and Gering E 1993 *Physica* B **190** 92
[26] Svane A 1996 *Phys. Rev.* B **53** 4275
[27] Hamann D R, Wu X, Rabe K M and Vanderbilt D 2005 *Phys. Rev.* B **71** 035117
[28] Reese R A, Sinha S K and Peterson D T 1973 *Phys. Rev.* B **8** 1332
[29] Baroni S, de Gironcoli S, Corso A D and Giannozzi P 2001 *Rev. Mod. Phys.* **73** 515
[30] Gonze X 1997 *Phys. Rev.* B **55** 10337
[31] Gonze X and Lee C 1997 *Phys. Rev.* B **55** 10355
[32] McMahon M I and Nelmes R J 1997 *Phys. Rev. Lett.* **78** 3884